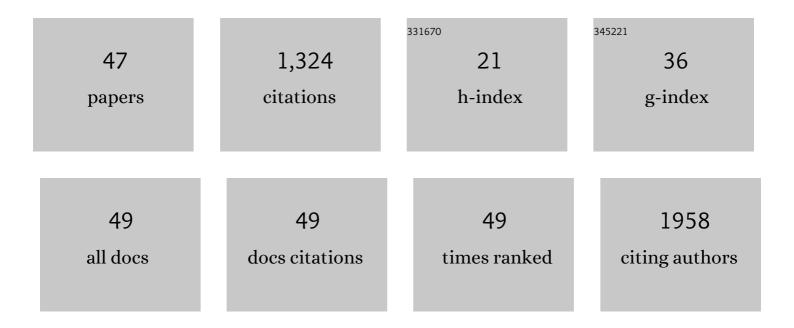
Marcela B FernÃ;ndez Van Raap

List of Publications by Year in descending order

Source: https://exaly.com/author-pdf/1228233/publications.pdf Version: 2024-02-01



#	Article	IF	CITATIONS
1	Small-angle X-ray scattering to quantify the incorporation and analyze the disposition of magnetic nanoparticles inside cells. Journal of Colloid and Interface Science, 2022, 608, 1-12.	9.4	3
2	Facile synthesis by laser ablation in liquid of nonequilibrium cobalt-silver nanoparticles with magnetic and plasmonic properties. Journal of Colloid and Interface Science, 2021, 585, 267-275.	9.4	29
3	Kinetically Stable Nonequilibrium Goldâ€Cobalt Alloy Nanoparticles with Magnetic and Plasmonic Properties Obtained by Laser Ablation in Liquid. ChemPhysChem, 2021, 22, 657-664.	2.1	15
4	Sciatic nerve regeneration after traumatic injury using magnetic targeted adipose-derived mesenchymal stem cells. Acta Biomaterialia, 2021, 130, 234-247.	8.3	24
5	Biocompatible Iron–Boron Nanoparticles Designed for Neutron Capture Therapy Guided by Magnetic Resonance Imaging. Advanced Healthcare Materials, 2021, 10, e2001632.	7.6	24
6	4D Multimodal Nanomedicines Made of Nonequilibrium Au–Fe Alloy Nanoparticles. ACS Nano, 2020, 14, 12840-12853.	14.6	53
7	Fluorescent and magnetic stellate mesoporous silica for bimodal imaging and magnetic hyperthermia. Applied Materials Today, 2019, 16, 301-314.	4.3	36
8	A simple and "green―technique to synthesize long-term stability colloidal Ag nanoparticles: Fs laser ablation in a biocompatible aqueous medium. Materials Characterization, 2018, 140, 320-332.	4.4	19
9	Nanoclusters of crystallographically aligned nanoparticles for magnetic thermotherapy: aqueous ferrofluid, agarose phantoms and <i>ex vivo</i> melanoma tumour assessment. Nanoscale, 2018, 10, 21262-21274.	5.6	33
10	Synthesis and Characterization of Magnetic Nanoparticle Colloids Generated in Liquid Media by UPLAâ€. , 2018, , .		0
11	Anticipating hyperthermic efficiency of magnetic colloids using a semi-empirical model: a tool to help medical decisions. Physical Chemistry Chemical Physics, 2017, 19, 7176-7187.	2.8	12
12	Optical and Magnetic Properties of Fe Nanoparticles Fabricated by Femtosecond Laser Ablation in Organic and Inorganic Solvents. ChemPhysChem, 2017, 18, 1192-1209.	2.1	30
13	Nanoscale Dielectric Function of Fe, Pt, Ti, Ta, Al, and V: Application to Characterization of Al Nanoparticles Synthesized by Fs Laser Ablation. Plasmonics, 2017, 12, 1813-1824.	3.4	4
14	Hybrid nanomaterials based on gum Arabic and magnetite for hyperthermia treatments. Materials Science and Engineering C, 2017, 74, 443-450.	7.3	55
15	Portable electromagnetic field applicator for magnetic hyperthermia experiments. , 2017, , .		1
16	Dipolar interaction and demagnetizing effects in magnetic nanoparticle dispersions: Introducing the mean-field interacting superparamagnet model. Physical Review B, 2017, 95, .	3.2	38
17	Magnetically Assembled SERS Substrates Composed of Iron–Silver Nanoparticles Obtained by Laser Ablation in Liquid. ChemPhysChem, 2017, 18, 1026-1034.	2.1	31
18	Effects of Nanostructure and Dipolar Interactions on Magnetohyperthermia in Iron Oxide Nanoparticles. Journal of Physical Chemistry C, 2016, 120, 12796-12809.	3.1	49

Marcela B FernÃindez Van

#	Article	IF	CITATIONS
19	Impact of magnetite iron oxide nanoparticles on wheat (Triticum aestivum L.) development: Evaluation of oxidative damage. Environmental and Experimental Botany, 2016, 131, 77-88.	4.2	144
20	Stress-Induced Gene Expression Sensing Intracellular Heating Triggered by Magnetic Hyperthermia. Journal of Physical Chemistry C, 2016, 120, 7339-7348.	3.1	19
21	Effect of Nanoclustering and Dipolar Interactions in Heat Generation for Magnetic Hyperthermia. Langmuir, 2016, 32, 1201-1213.	3.5	126
22	Ag nanoparticles formed by femtosecond pulse laser ablation in water: self-assembled fractal structures. Journal of Nanoparticle Research, 2015, 17, 1.	1.9	25
23	Synthesis of Ni Nanoparticles by Femtosecond Laser Ablation in Liquids: Structure and Sizing. Journal of Physical Chemistry C, 2015, 119, 13184-13193.	3.1	48
24	Structure, configuration, and sizing of Ni nanoparticles generated by ultrafast laser ablation in different media. Proceedings of SPIE, 2015, , .	0.8	0
25	Quasi-static magnetic measurements to predict specific absorption rates in magnetic fluid hyperthermia experiments. Journal of Applied Physics, 2014, 115, .	2.5	22
26	Influence of size-corrected bound-electron contribution on nanometric silver dielectric function. Sizing through optical extinction spectroscopy. Journal Physics D: Applied Physics, 2013, 46, 435301.	2.8	27
27	Stability and Relaxation Mechanisms of Citric Acid Coated Magnetite Nanoparticles for Magnetic Hyperthermia. Journal of Physical Chemistry C, 2013, 117, 5436-5445.	3.1	161
28	Structural and magnetic study of zinc-doped magnetite nanoparticles and ferrofluids for hyperthermia applications. Journal Physics D: Applied Physics, 2013, 46, 125006.	2.8	51
29	Analysis of the structure, configuration, and sizing of Cu and Cu oxide nanoparticles generated by fs laser ablation of solid target in liquids. Journal of Applied Physics, 2013, 113, .	2.5	46
30	Self organization in oleic acid-coated CoFe2O4 colloids: a SAXS study. Journal of Nanoparticle Research, 2012, 14, 1.	1.9	23
31	Size dependent Cu dielectric function for plasmon spectroscopy: Characterization of colloidal suspension generated by fs laser ablation. Journal of Applied Physics, 2012, 112, .	2.5	16
32	A quasi-continuous observation of the α-transition of Fe1 + x S by Mössbauer line tracking. Hyperfine Interactions, 2010, 195, 161-165.	0.5	7
33	Experimental design and methodology for a new Mössbauer scan experiment: absorption line tracking. Hyperfine Interactions, 2009, 188, 137-142.	0.5	12
34	Mössbauer effect phase determination in iron oxide–polyaniline nanocomposites. Hyperfine Interactions, 2007, 179, 81-86.	0.5	1
35	Magnetic and thermal Mössbauer effect scans: a new approach. Hyperfine Interactions, 2006, 167, 839-844.	0.5	6
36	Detailed magnetic dynamic behaviour of nanocomposite iron oxide aerogels. Journal of Physics Condensed Matter, 2005, 17, 6519-6531.	1.8	20

Marcela B FernÃindez Van

#	Article	IF	CITATIONS
37	Hyperfine field temperature dependence of Fe3Si from Mössbauer thermal scans. Physica B: Condensed Matter, 2004, 354, 369-372.	2.7	13
38	Small-angle x-ray scattering study of nanocrystalline FeyCu1-yalloys produced by ball milling. Journal of Physics Condensed Matter, 2002, 14, 857-864.	1.8	4
39	Hyperfine Field and Isomer Shift Evolution in Hydrogenated Nd–Fe–B Alloy. Hyperfine Interactions, 2001, 134, 123-129.	0.5	Ο
40	Kinetic aspects of the solid hydrogenation– disproportionation–desorption–recombination process in Nd13.67Co15.74Al0.77Ga0.27Zr0.03Fe62.2B7.33 alloys. Journal of Applied Physics, 1998, 84, 3786-3791.	2.5	0
41	Mössbauer study of the Fe-Si phases produced by Fe implantation followed by ion-beam-induced epitaxial crystallization. Physical Review B, 1996, 54, 12787-12792.	3.2	16
42	$M ilde{A}\P$ ssbauer characterization of \hat{I}^3 -FeSi2precipitates in Si(100). Physical Review B, 1995, 51, 86-90.	3.2	14
43	On the microstructure and thermal stability of rapidly quenched Fe–B alloys in the intermediate composition range between the crystalline and amorphous states. Journal of Materials Research, 1995, 10, 1917-1926.	2.6	7
44	Anisotropic Phase Separation through the Metal-Insulator Transition in Amorphous Alloys. Physical Review Letters, 1994, 73, 1118-1121.	7.8	25
45	Structural dependence on composition of rapidly quenched Fe-B alloys. Physical Review B, 1992, 46, 13881-13888.	3.2	13
46	Structural composition dependence of amorphous silicon-iron prepared by ion implantation and by coevaporation: A Mössbauer study. Physical Review B, 1991, 44, 4290-4295.	3.2	18
47	Mössbauer study of the thermally induced transformation of the Fe0.91B0.09rapidly quenched crystalline alloy, Journal of Applied Physics, 1989, 66, 875-880	2.5	4